Emergence of One-Dimensional Physics in the Distorted Shastry-Sutherland Lattice

M. Moliner,[1, *] I. Rousochatzakis,[2, †] and F. Mila[3, ‡]

[1]*Institut für Nanotechnologie, Karlsruhe Institute of Technology, 76344 Eggenstein-Leopoldshafen, Germany.*
[2]*Max-Planck-Institut für Physik komplexer Systeme, Nötnitzer Straße 38, 01187 Dresden, Germany.*
[3]*Institute of Theoretical Physics, Ecole Polytechnique Fédérale de Lausanne, CH-1015 Lausanne, Switzerland.*
(Dated: April 30, 2018)

Motivated by the on-going investigation of $SrCu_2(BO_3)_2$ under pressure, we study a variant of the two-dimensional Shastry-Sutherland (SS) spin-1/2 model with two types of dimers. Combined with the frustration of the SS model, this modification induces, in a large parameter range, a dimensional reduction at low energies, with nearly decoupled effective $S = 1$ Haldane chains forming along one of the diagonals of the lattice. We also present evidence that the intermediate plaquette solid phase of the undistorted SS model remains stable in a finite region of the phase diagram.

Introduction.— An exciting route for exploring new phases in frustrated magnets consists in applying hydrostatic pressure so as to considerably modify the dominant magnetic interactions and thus alter the relevant low-energy degrees of freedom. The quasi-2D compound $SrCu_2(BO_3)_2$ [1] offers such a possibility since it is in the close vicinity of a quantum phase transition from an exact tensor product of singlets toward a plaquette solid[2, 3]. Indeed, Nuclear Magnetic Resonance (NMR)[4, 5], Inelastic Neutron Scattering (INS)[6], as well as earlier susceptibility measurements[7], show strong evidence that $SrCu_2(BO_3)_2$ undergoes at least one phase transition under high hydrostatic pressure, the nature of which is still not fully understood. What is clear however is that the four-fold (C_4) symmetry around the void plaquettes is quickly lost under pressure, so that nearest-neighbor dimers pointing in different directions become inequivalent (see Fig.1). This naturally leads to an extension of the Shastry-Sutherland (SS) model with two different diagonal bonds J_1 and J_2 described by the spin $S = 1/2$ Heisenberg Hamiltonian

$$\mathcal{H} = J' \sum_{\langle ij \rangle} \mathbf{S}_i \cdot \mathbf{S}_j + J_1 \sum_{\ll ij \gg_1} \mathbf{S}_i \cdot \mathbf{S}_j + J_2 \sum_{\ll ij \gg_2} \mathbf{S}_i \cdot \mathbf{S}_j \quad (1)$$

where J' denotes the nearest-neighbor exchange (see Fig. 1). Since all nearest-neighbor bonds J' are equal, the product of singlets on J_1 and J_2 bonds is always an eigenstate, as it is for the undistorted SS model. Besides, although the C_4 symmetry is lost, both the sets of J_1 and J_2 bonds form a square lattice. It thus seems natural to expect that the phase diagram will consist of three phases, as for the regular SS model: the exact singlet phase for small J', the Néel phase for large J', and an intermediate plaquette phase with 2D character[2, 3].

In this paper, using a variety of analytical and numerical techniques, we show that making the diagonal bonds inequivalent actually triggers an abrupt dimensional reduction into a new, effectively 1D Haldane phase in a wide parameter range (see Fig. 2). In this phase the effective low-energy physics can be described in terms of nearly decoupled, fully frustrated 2-leg ladders (see Fig. 1) running along one of the two diagonals of the square lattice. Remarkably enough, the spins on the J_2-bonds form *triplets* in this phase, leading to a com-

pletely different picture of the low-lying magnetic excitations as compared to the exact singlet phase.

The emergence of this new singlet phase is best understood by starting from the limit $J_2/J_1 = J'/J_1 = 0$. The model then reduces to a set of isolated dimers on the J_1-bonds and isolated free spins on the remaining sites (see Fig. 1), resulting into a macroscopically degenerate ground state manifold. The degeneracy is lifted by switching on the inter-dimer coupling J' which, to leading (second) order, *a priori* couples a given spin to 12 neighbors (see Fig. 1, where the 12 neighbors of site 0 are numbered from 1 to 12). Each second-order process involves an intermediate state with a J_1 dimer in a triplet state, and the resulting coupling is ferromagnetic and of amplitude $-J'^2/2J_1$ if the J' bonds are connected to the same site of the J_1 dimer, while it is antiferromagnetic and of amplitude $J'^2/2J_1$ if they are connected to opposite sites. When processes with different signs couple two spins, they cancel out due to quantum interferences. As a result, the couplings between site 0 and sites 6 to 12 vanish, and site 0 is only
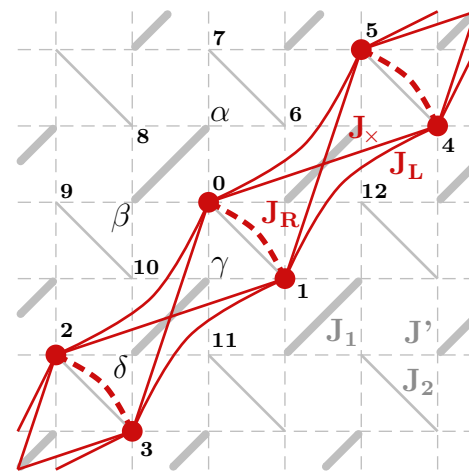

FIG. 1: (color online) The distorted SS model (thick and thin gray lines for J_1, J_2, and dashed for J') of this work, together with the effective quasi-1D model (red solid and dashed thick lines) emerging in the limit $J_1 \gg J_2, J'$ which gives rise to the Haldane phase.
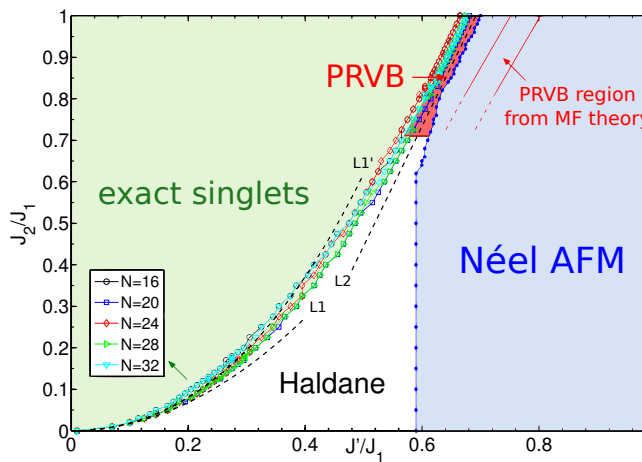
FIG. 2: (color online) The phase diagram of the present model obtained by exact diagonalizations (symbols with lines). The r lines enclose the stability region of the PRVB phase as obtained fro the quadrumer boson operator method (see text). The dashed lin L1 and L1' denote the boundary between the exact dimer and t Haldane phase as obtained from perturbation theory up to second and third orders, while the dashed line L2 is the line along which we examine the low-E spectrum shown in Fig. 5 below.
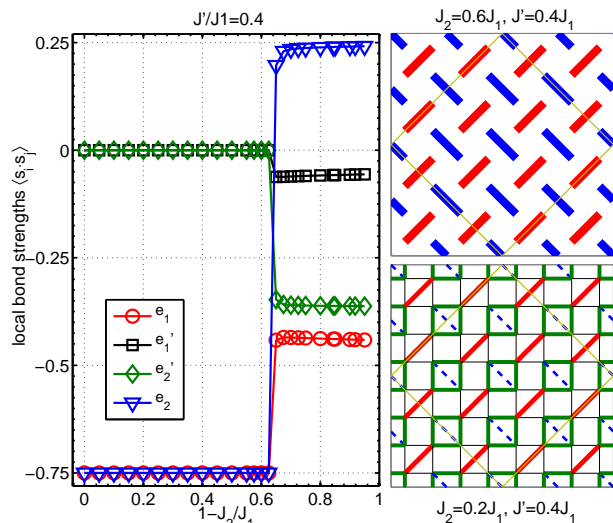

FIG. 3: (color online) Left panel: Ground state expectation values of the four different nearest-neighbor exchange energies $\mathbf{S}_i \cdot \mathbf{S}_j$ for the 32-site cluster ($e_{1,2}$ for the $J_{1,2}$ diagonal bonds, and $e'_{1,2}$ for J'-bonds on plaquettes which contain $J_{1,2}$ bonds). Right panels: The corresponding local energy profiles for representative cases inside the exact singlet state (above) and the Haldane state (below). Positive (negative) exchange values are shown by dashed (solid) lines, whose width is proportional to the magnitude of these values.

coupled to its neighbors on the ladder shown in Fig. 1. The couplings between site 0 and sites 2, 3, 4 and 5 are all anti-ferromagnetic and of amplitude $J'^2/2J_1$, while the coupling between 0 and 1 is ferromagnetic and equal to $-J'^2/J_1$.

Including both J_2 and J', and up to second order in J'/J_1, our 2D model thus reduces to an infinite set of 2-leg, frustrated spin ladders directed along the J_1 diagonal bonds. The effective interactions within the ladders are depicted in Fig. 1 on top of the original model. They consist of the rung coupling $J_R = J_2 - J'^2/J_1$, the leg coupling $J_L = J'^2/2J_1$, and a frustrating coupling $J_\times = J_L$. This model has been studied quite extensively[8, 9]. It has the special property that the total spin on each rung is a good quantum number, which allows to determine a large number of eigenstates exactly[8]. In particular, in the limit $J_R \gg J_L$ (or $J_2 \gg J'^2/J_1$) the low-est energy is obtained by minimizing the number of triplets in the rungs[10]. The resulting ground state of the ladder is the product of rung singlets, which together with the strong J_1 singlets correspond to the exact orthogonal-dimer phase of the SS model. On the contrary, if J_R is not too large (and a fortiori if it is negative), fluctuations between neighboring triplets dominate and the lowest energy is obtained by plac-ing a triplet on each rung. The ladder then behaves like a spin-1 chain, and hence the ground state corresponds to the Haldane gapped phase[11]. The actual transition between the exact dimer and the Haldane phase is known[8] to take place at $J_R/J_L \simeq 1.4$ and it is of first order. Rewritten in terms of the original couplings of our model, this boundary corre-sponds to the line $J_2 = 1.7\,J'^2/J_1$, which is shown by the dashed line L1 in Fig. 2. The dashed line L'1, defined by $J_2 = 1.7J'^2/J_1 + 1.55J'^3/J_1^2$, corresponds to the bound-ary obtained from perturbation theory up to third order[17].

Third order processes in J'/J_1 also induce some coupling be-tween nearest and next-to-nearest neighboring ladders, result-ing into a complex network[18], but the quasi-1D character of the (short-range) spin correlations and the finite spin gap seem to be a robust feature of this phase, as suggested by exact di-agonalizations.

Exact diagonalizations.— To determine the behavior of the present model away from the above perturbative regime and to accurately obtain the full phase diagram of the model, we have performed an extensive exact diagonalization study (ED) on finite-size clusters with periodic boundary conditions. Apart from U(1) spin rotations and translational invariance we have also exploited the two reflection symmetries (denoted here by $\mathcal{R}_1$ and $\mathcal{R}_2$) along the two diagonals of the square lattice.

The transition between the exact singlet phase and the Hal-dane phase is most simply identified by measuring the ground state spin-spin correlations $\langle \mathbf{S}_i \cdot \mathbf{S}_j \rangle$ on neighboring bonds, as shown in Fig.3: they are rigorously equal to $-3/4$ on dimer bonds and to zero on J' bonds in the exact dimer phase, and jump upon entering the Haldane phase to ferromagnetic and nearly equal to $1/4$ on the J_2 bonds, and to intermediate anti-ferromagnetic values on J_1 and J' bonds. The resulting first order transition lines shown in Fig. 2 are in good agreement with the perturbative predictions and show a weak system size dependence. In addition, the correlation profiles shown in the right panels of Fig. 3 demonstrate how the 2D-lattice decou-ples into almost non-interacting 2-leg ladders.

Next, we examine the behavior of the spin gap by look-ing at the evolution of the low-energy excitation spectrum as

we move away from the exact dimer into the Haldane phase. Figure 4 shows the low-energy spectrum of the 32-site cluster along the line $J' = 0.4J_1$ in the $S_z = 0$ and 1 sectors. All energies are measured from the ground state. In the exact dimer phase the spin gap scales linearly with J_2 and thus decreases as we go towards the Haldane phase. This happens because a magnetic $S = 1$ excitation results by promoting a rung singlet[19] into a triplet which costs energy J_2 (disregarding the polarization corrections to the spin gap driven by J'[1]). By contrast when entering the Haldane phase at $J_2 \simeq 0.365J_1$ the gap does not change with J_2 any longer. This happens because once we pay the energy to form the effective spin-1 entities on the rungs the energy scale J_2 does not enter their effective dynamics any longer.

The 1D character of the Haldane phase underlies also a number of striking spectral features in the singlet sector. In particular, Fig. 4 shows a number of singlets (highlighted by dashed lines) which group together into almost degenerate levels, and all seem to become soft together with the Haldane state (red dashed line). These correspond to singlets where not all ladders are in the Haldane phase. Specifically, the 32-site cluster (enclosed by solid yellow lines in the right panels of Fig. 3) decomposes into four 2-leg ladders with two J_2-bonds each. To form the Haldane phase in a single ladder we pay energy $2J_2$ to create two triplets (disregarding again the polarization energy driven by J'), but we gain an energy δ_H from their interaction. This gives 4 possible states with energy $E_{1H} \simeq 2J_2 - \delta_H$ whereby one ladder has entered the Haldane phase but the remaining three have still singlets in their rungs. Similarly, there must exist: 6 states with two ladders in the Haldane phase and energy $E_{2H} \simeq 2E_{1H}$; 4 states with three ladders in the Haldane phase and $E_{3H} \simeq 3E_{1H}$; and finally a single state where all ladders are in the Haldane phase with $E_{4H} \simeq 4E_{1H}$. Both the multiplicities and the dependence on J_2 (the slope in the dashed lines of Fig. 4) are in agreement with the ED spectra. In addition, we have derived the decomposition of each group of singlets into irreducible representations of the space group of the 32-site cluster and the results also agree with the ED spectra. Finally, the fact that $E_{nH} \simeq nE_{1H}$ explains why the above groups of singlets seem to become soft together with the Haldane state.

We note here that the above energy considerations are only true to leading order in J'. There are various perturbative corrections which renormalize the energy of each of the above singlets in a different manner. For the 32-site cluster, it is the global Haldane state that crosses the exact singlet phase first.

Upon increasing J'/J_1, the Haldane phase undergoes a second order transition into the Néel phase. The disappearance of the Néel order is continuous and corresponds to the vanishing of the local moment m obtained by a usual[3] finite-size extrapolation $m_N \simeq m + \frac{c}{\sqrt{N}}$, using numerical data for the corresponding spin structure factor at zero momentum.[20] We find that for $J_2 \lesssim 0.6J_1$, the Néel boundary does not depend on J_2, which is related to the absence of this energy scale from the effective dynamics of the Haldane phase. On the other hand, the bending of the Néel boundary for $J_2 \gtrsim 0.6J_1$ indi-
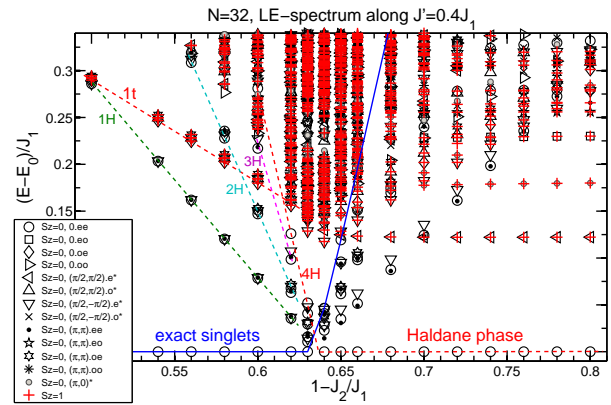

FIG. 4: (color online) Low-energy spectrum (measured from the GS) for the 32-site cluster along the line $J'/J_1 = 0.4$ in the $S_z = 0$ and 1 sectors. The blue solid line shows the energy of the exact singlet phase. The dashed lines highlight the n-Haldane chain singlets discussed in the text. The quantum numbers shown in the legends correspond to the allowed momenta of the 32-site cluster and the parities with respect to the two diagonal reflections $\mathcal{R}_{1,2}$.
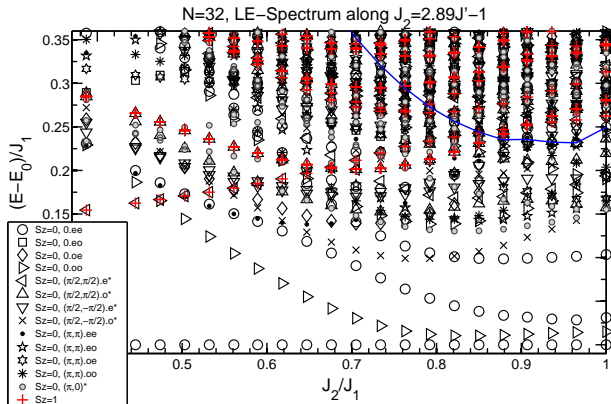

FIG. 5: (color online) Low-energy spectrum (measured from the GS) of the 32-site cluster along the line L_2 ($J2 = 2.89J' - 1$) of Fig. 2 in the $S_z = 0$ and 1 sectors. The solid (blue) line stands for the energy of the exact singlet phase.

cates the proximity to another phase, different from the Haldane one. We now show evidence, first by a detailed spectral analysis and then by a perturbative mean-field approach, that this phase is adiabatically connected to the plaquette phase present for $J_2 = J_1$[2, 3]. We begin by examining the evolution of the low-lying spectrum along the line L2 of Fig. 2. As shown in Fig. 5 for the 32-site spectrum, a low-energy excitation becomes gradually soft above $J_2/J_1 \sim 0.7 - 0.8$. This excitation has zero momentum but it has odd parity with respect to $\mathcal{R}_1$ and $\mathcal{R}_2$, in contrast to the ground state. If these two states become degenerate in the thermodynamic limit then the above quantum numbers are exactly the ones expected for the Z_2 plaquette phase, since the latter does not break translational invariance but it does break $\mathcal{R}_1$ and $\mathcal{R}_2$.

We also find a large number of singlets below the lowest triplet excitation. The majority of these states have a positive

curvature with J_2, similarly to the exact singlet state shown by the solid (blue) line. Hence these states are most probably adiabatically connected to singlets above the dimer phase, such as the ones we discussed above that must become nearly soft at the boundary with the Haldane phase (in addition there could also be some bound states of triplons[12]). In agreement with Läuchli et al. [3], we also find a singlet which lies slightly above the lowest two singlets at $J_2 = J_1$. The nature of this singlet might well be a singlet excitation (e.g. a domain wall) of the plaquette phase.

A complementary confirmation that the plaquette phase survives in a small region for $J_2 \neq J_1$ can be also given by an analytical mean-field approach based on quadrumer boson operators[3, 13–15]. Here, one essentially expands around the explicitly symmetry broken phase where every second void square is in the singlet ground state of an isolated Heisenberg plaquette[2]. The ground state and low-lying excitations of the original model are then approximated by truncating the Hilbert space of each plaquette to its singlet ground state and its lowest triplet, which is achieved by the bosonic representation of the four spins ($j = 1, \ldots 4$)

$$S_j^\alpha = \frac{(-1)^j}{\sqrt{6}} \left(s^\dagger t_\alpha + t_\alpha^\dagger s \right) - \frac{i}{4} \sum_{\beta,\gamma} \epsilon^{\alpha\beta\gamma} t_\beta^\dagger t_\gamma, \quad (2)$$

where $\alpha = x, y, z$, and $s^\dagger$, $t_\alpha^\dagger$ create respectively the singlet ground state and the lowest triplet excitation of a single Heisenberg plaquette. A hard-core constraint restricts the boson occupation number of each plaquette $s^\dagger s + \sum_\alpha t_\alpha^\dagger t_\alpha = 1$ so that the bosonic representation obeys the spin algebra. The energy of a single plaquette becomes $\mathcal{H}_P = E_s s^\dagger s + E_t \sum_\alpha t_\alpha^\dagger t_\alpha$. Following the standard procedure[3, 14, 15], we obtain a triplet mode with dispersion (in units of $J_1 = 1$)

$$\omega^2(\mathbf{k}) = J'^2 + \frac{2}{3}J'\left[(1-2J')\cos k_x + (J_2-2J')\cos k_y \right] \quad (3)$$

For $J' > \frac{1}{2}J_1$ and $J_2 < 2J'$ the minimum of the spectrum is at $\mathbf{k} = 0$ and this becomes soft along the line $J_2 = -1 + \frac{5}{2}J'$, which corresponds to the Néel ordering. The first-order transition line between the dimer and the plaquette phase is obtained by comparing the exact dimer energy with that of the plaquette state including the zero-point motion from the quadratic terms. These lines are depicted as red lines in Fig. 2. The stability region is shifted to larger J'/J, as already observed for the standard SS model, but the slopes are in good agreement with ED. Note that the first order boundary between the plaquette and the Haldane phase cannot be found with our method since we do not have an expression for the ground state energy of the Haldane phase.

Conclusion.— We have introduced a variant of the SS model with two types of diagonal couplings as a minimal model for the loss of the C_4 symmetry in SrCu$_2$(BO$_3$)$_2$ under high pressure. We find a novel quasi-1D Haldane phase

where the low-energy physics can be described in terms of fully frustrated decoupled 2-leg ladders which form $S = 1$ entities on their rungs. When J_2/J_1 decreases, the gap to the first excitation first decreases linearly, and then levels off after crossing the boundary between the exact dimer phase and the Haldane phase. Assuming that the main effect of pressure is to reduce the ratio J_2/J_1, this is precisely what has been reported by INS[6], as well as by NMR[16] for the nonmagnetic sites. However, the presence of magnetic sites possibly arranged on every second ladder, as suggested by NMR[5], and of a low-lying excitation below the excitation that levels off, as revealed by INS[6], goes beyond the prediction of the present model and requires further investigation.

* Electronic address: Marion.Moliner@kit.edu
† Electronic address: rousocha@pks.mpg.de
‡ Electronic address: Frederic.Mila@epfl.ch

[1] S. Miyahara and K. Ueda, J. Phys.: Condens. Matter **15**, R327 (2003).
[2] A. Koga and N. Kawakami, Phys. Rev. Lett. **84**, 4461 (2000).
[3] A. Laeuchli, S. Wessel, and M. Sigrist, Phys. Rev. B **66**, 014401 (2002).
[4] M. Takigawa, T. Waki, M. Horvatić, and C. Berthier, J. Phys. Soc. Jpn. **79**, 011005 (2010).
[5] T. Waki *et al.* , J.Phys. Soc. Jpn **76**, 073710 (2007).
[6] M. Zayed *et al.* , private communication.
[7] H. Kageyama *et al.* , Physica B **329-333**, 1020 (2003).
[8] A. Honecker, F. Mila, and M. Troyer, Eur. Phys. J. B **15**, 227 (2000).
[9] N. B. Ivanov, and J. Richter, Physics Letters A **232**, 308 (1997).
[10] I. Bose and S. Gayen, Phys. Rev. B **48**, 10653 (1993).
[11] F. D. M. Haldane, Phys. Rev. Lett. **50**, 1153 (1983).
[12] C. Knetter, A. Bühler, E. Müller-Hartmann, and G. S. Uhrig, Phys. Rev. Lett. **85**, 3958 (2000).
[13] R. N. Bhatt and S. Sachdev, Phys. Rev. B **41**, 9323 (1990).
[14] M. E. Zhitomirsky and K. Ueda, Phys. Rev. B **54**, 9007 (1996).
[15] O. A. Starykh and A. Furusaki and L. Balents, Phys. Rev. B **72**, 094416 (2005).
[16] M. Takigawa *et al.* , private communication.
[17] Up to third order, the effective ladder couplings are $J_R = J_2 - J'^2/J_1 - \frac{1}{2}J'^3/J_1^2$ and $J_L = J_\times = \frac{1}{2}J'^2/J_1 + \frac{3}{4}J'^3/J_1^2$.
[18] Site 0 couples to 6 and 10 through J'^3/J_1^2, and to 7, 9, 11 and 12 through $\frac{1}{2}J'^3/J_1^2$. Site 0 is also coupled to site 8 belonging to the next-nearest-neighbor ladder through J'^3/J_1^2.
[19] We note here that a triplon excitation prefers to sit on the J_2-bonds since $J_2 < J_1$.
[20] For the Néel boundary $J'_{cr}(J_2)$ of Fig. 2 we made an unbiased use from all clusters with 16, 20, 24, 28, and 32 sites. Using the most symmetric clusters (16 and 32 sites) shifts J'_{cr} by no more than a few percent.